International Journal of Research in Engineering and Innovation (IJREI)
journal home page: http://www.ijrei.com
ISSN (Online): 2456-6934

ORIGINAL ARTICLE

Optimization of process parameters of friction stir welded joint of dissimilar aluminum alloy AA5083 and AA6082

Muzamil Farooq, Amit Gupta, Vikas Nandal

Department of Mechanical Engineering Geeta Engineering College, Naultha, Panipat, India

Article Information

Received: 25 August 2020
Revised: 19 September 2020
Accepted: 21 October 2020
Available online: 11 November 2020

Keywords:

Tensile strength;
Microhardness;
Residual Stress;
Optimization;
Friction stir welding;

Abstract

In this investigation central composite design (CCD) technique and mathematical model was developed by response surface methodology with three parameters, four levels and 20 runs, was used to develop the relationship between the FSW parameters (rotational speed, traverse speed, and tilt angle) and the responses (tensile strength, % Elongation, micro-hardness and residual stress) of dissimilar aluminum alloys AA5083 and AA6082 were established. The maximum tensile strength (214 MPa) was found at tool rotation speed 1300 rpm, traverse speed 45 mm/min with tilt angle 1^0. The maximum micro-hardness (86 HV) was found at tool rotation speed 1300 rpm, traverse speed 45 mm/min with tilt angle 1^0. The minimum tensile strength (161 MPa) was observed at tool rotation speed 1000 rpm, traverse speed 30 mm/min with tilt angle 2^0. In addition, a numerical model and empirical relationship was developed by design expert software between processing parameters (tool rotation speed, traverse speed, and tilt angle) and response surface parameters (tensile strength, percentage elongation and micro-hardness at nugget zone) and the optimized value of tensile strength, % elongation, micro-hardness, and residual stress were observed as 187.6 MPa, 19.93, 78.39 HV and 22.02 MPa respectively.

1. Introduction

Welding is a precise, reliable and cost effective technique used for joining of ferrous and non-ferrous metals. It is widely used because of the high strength of the welded joint when compared to other joining methods like riveting, fastening, adhesive bonding. Welding is an indispensable joining technology (for both fabrication and repair works) used in manufacturing industries, such as automotive, aerospace, ship building, power generation, petroleum production and refining, construction and farm equipment, electronics, and medical devices. The friction stir welding (FSW) is an energy efficient, and eco-friendly solid state welding process invented in 1991 in England as shown in fig.1.

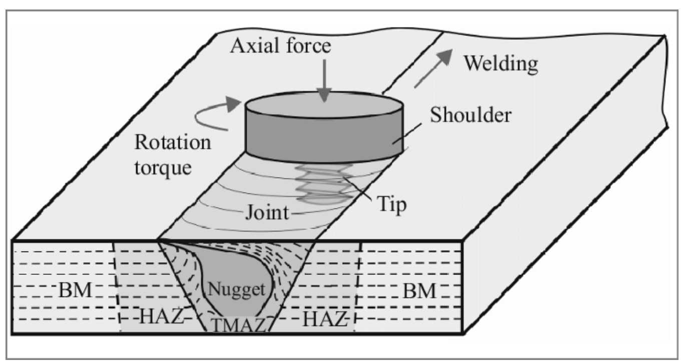

Figure 1: Friction Stir Welding

Corresponding author: Muzamil Farooq
Email Address: bhatermuzamil@gmail.com
https://doi.org/10.36037/IJREI.2021.5102

The effect of welding parameters on the structure and properties of the nugget zone in AA7010 was investigated and it was found that there is an optimum rotational speed, for a given traverse speed, that gives the highest strength and ductility for the nugget zone. As the traverse speed is increased, it is necessary to increase the rotational speed to maintain this optimum condition. For a given traverse speed, there is a significant variation in grain size and hardness from the top to the bottom of the welds [1]. Martial flow in the weld zone is non symmetrically side distributed about the weld line because the material flow during friction stir welding is mainly controlled by both advancing and rotating speeds [2]. The optimal processing parameters for producing a defect free weld when a rotating threaded weld tool is inserted into a weld and literally stirs the edges of the seam together. The lead wire embedded in the weld seam as a tracer. At the welding temperature of aluminum, the lead becomes molten and is continuously carried with the macro-flow of the weld metal. A through thickness flow of metal was revealed in the X-rat imaging of the lead tracer in addition to revealing a cycle oscillation in the plasticized metal affected by the process [3]. The tensile strength is directly proportional to traverse speed (TS). Softening of the material was observed in the weld region and mostly evident in the heat-affected zone (HAZ) on the advancing side of the welds and corresponded to the failure location in tensile tests. The reason for this phenomenon is due to the kinetic and thermal asymmetry of the FSW process [4]. The New welding approach has been introduced to improve the weldeing quality of TIG welded joint, the influence of friction stir processing on TIG welded joint have been analyzed and they observed mechanical properties and heat transfer of TIG+FSP welded joint. The mechanical properties of TIG+FSP welded joint were observed better than TIG welded joints. [5-11]. The tensile strength of the joint is lower than that of the base metal. Decrease in hardness in the weld region and tunnel defect were observed at the intersection of SZ and thermo-mechanically affected zone (TMAZ) due to high rotational speed and traverse speed. Also, the welded samples did not fail in bend test [12]. The effect of process parameters on the joint performance was studied and found that 1600 rpm and 225 mm/min gave 2.8 mm penetration for 3 mm thick workpieces with 4 mm tool root diameter, and the 3 mm tip diameter [13]. The failure occurred at a much lower load during tensile loading than during shear loading. Also, the authors presented experimental data on load carrying capacities and fatigue of dissimilar aluminium-alloy FSW welds [14]. The mechanical property variations in AA3003-H24 and 2124/Sic/25p–t4 alloy joints at rotational speed of 900 rpm and traverse speed of 125 mm/min. It was found that the maximum tensile strength is about 182 MPa. And, the hardness across the weld nugget varies and a minimum value occurred on retreating side of the HAZ [15]. The rotational speed and welding feed rate are the factors that have greater influence on hardening parameters The numerical models response surface hardening models (RSHM) were compared with those through least square hardening models (LSHM) and confronted to the experimental results. Indeed, within the limit of a relative average deviation of about 9.3%, between the experimental model and numerical models expressed in terms of tension-elongation, the validity of these models is acceptable [16]. The experiments with and without silicon carbide powder and analyzed the effect of RS in the range of 600-1200 rpm and TS in the range of 36-72 mm/min. The optimal values were found at 1200 rpm, 72 mm/min and axial load of 8 kN. Also, it was found that maximum hardness occurred at the centre of the weld as compared to other zones of weld joint and is attributed to intensive stirring process [17]. The joining of dissimilar aluminum-alloys (AA6262-T6 and AA7075-T6) by varying the weld process parameters (tool rotational speed, weld speed and axial force) with cylindrical tool-pin profile have been analyzed and they concluded that better mechanical properties (hardness and tensile strength) are obtained with the FSW plate welded with 1200 rpm, 36 mm/min and 9kN axial force as compared with other range of values. The main idea of this research was to study the joining of dissimilar materials AA5083 and AA6082 using the friction stir welding method. The objective of present work is to optimize the process parameters such as tool rotational speed, traverse speed and tilt angle for obtaining the greater or optimum value of mechanical properties like ultimate tensile strength, micro-hardness and residual stress of the friction stir welded joint of AA6082 and AA5083.

2. Materials and method

The work-pieces to be joined by FSW process are machined to the required dimensions. The required dimensions of the plates are prepared based on the bed length and width of the milling machine, length of the backing plate, and the design of the clamping system, so that the arrangements do not allow the distortion of the plates due to forces induced by the rotating tool. However, the aluminum-alloys are designed to be around 300 mm long and 80 mm wide sheet metal cut into the specified dimensions by a shear cutting technique. The final dimensions of the work pieces are 150 mm x 40 mm x 6.2 mm. The aluminum plates were to be machined at the sides in order to make them flat to ensure accurate face-to-face contact at weld joint. This was accomplished by using the shaping machine and a vice for holding the plates firmly. The experiments are developed by design expert software. Three factor and three response surface design matrix was developed with 20 experiments. Mathematical modelling was carried out by response surface method (RSM) and optimum value was opting with RSM results. The chemical composition of base plate and design of experiments is shown in table 1 and 2.

Table 1: Chemical composition of base material

Al- alloy	Si	Fe	Cu	Mn	Mg	Cr	Zn	Ti	Al
AA5083	0.4	0.3	0.2	0.6	4.5	0.1	0.2	0.1	Bal
AA6082	1.2	0.2	0.1	0.4	0.6	0.2	0.3	0.2	Bal

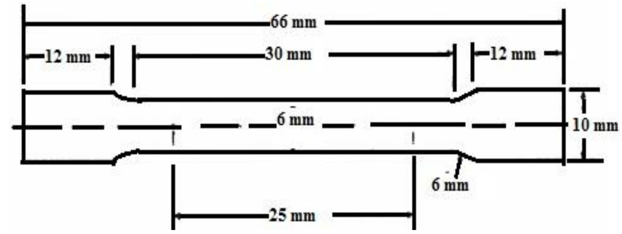

Figure 2: Dimension of tensile test specimen

The tensile stress of friction stir welded joints were measured under uniaxial tensile stress with the help of universal testing machine as per ASTM E8 standard as shown in fig. 2.

Table 2: Process parameters of friction stir welding

Run	A:Tool Rotation Speed (rpm)	B:Traverse speed (mm/min)	C:Tilt Angle (º)
1	1150	45	2
2	1300	30	0
3	1150	45	0
4	1000	30	0
5	1150	45	1
6	1000	60	2
7	1300	45	1
8	1150	45	1
9	1150	45	1
10	1300	60	0
11	1150	45	1
12	1000	60	0
13	1150	30	1
14	1150	45	1
15	1000	45	1
16	1300	60	2
17	1150	60	1
18	1000	30	2
19	1150	45	1
20	1300	30	2

3. Results and discussion

3.1 Tensile strength

The optimum combination of processing parameters has been selected with the help of design expert software. There are 20 experiments have been done on the basis of processing parameters. The optimum processing parameters and their responses have been shown in table 3. The mechanical properties like ultimate tensile strength (UTS), % elongation, and micro-hardness of the FSW joints of AA 5083 and AA6082 with different RS and TS are studied from the experimental results and are discussed below in detail. Table 3 gives the summary of measured ultimate tensile strength (UTS), % elongation, microhardness and residual stress of the FSW joints of AA 5083 and AA6082. It can be observed that % elongation increased with increasing rotational speed, as expected because hardness increases (see Fig.4). Also, the tensile strength increased slightly with increasing rotational speed.

At same rotational speed, the tensile strength decreased with increasing traverse speed. However, the tensile strength and mean hardness of FSW joint are closer to the base metal values at 1300 rpm and 45 mm/min with tilt angle 1° and therefore considered to be optimum process parameters. Based on the observed trends, it can be concluded that there should be a trade-off between tensile strength and hardness while selecting the optimum process parameters. When the rotational speed increased, the heat input per unit length of the welded joint also increased which caused a fine uniform grain refinement was obtained to improve the tensile strength. When the tool rotational speed increases from 1300 rpm may produce an excessive release of stirred welded material on the top surfaces of the base plate, obtained micro void into the stirred zone.

The tensile strength of welded joints was varied between 161-214 MPa. The minimum tensile strength (161 MPa) was observed at tool rotation 1000 rpm, traverse speed 30 mm/min with tilt angle 2º, whereas maximum tensile strength was observed at at tool rotation 1300 rpm, traverse speed 45 mm/min with tilt angle 1º as shown in fig. 3.

The increase in temperature as well as coarsening of grains and cooling rate at more than desired temperature may reduce the tensile strength of the welded joint of at high traverse speed. Some defects were observed when the material flow around the advancing side (A.S) of the weldment, because there is no force promoting its movement back into the volume stirred by the moving tool [18]. All the fracture occurred at the interface or near the nugget zone (NZ) and thermo mechanically affected zone (TMAZ) on the advancing side (AS). The reason of fracture near to the nugget zone and thermo mechanically affect zone may be resulting in many coarse grains brittle structure near to the NZ and TMAZ [19]. It may be noted that the all joints are fractured at the advancing side, this shows that the tensile strength of these weldment are not same on both side to the weld center, it means the strength of advancing side is weaker than the retreating side (RS).

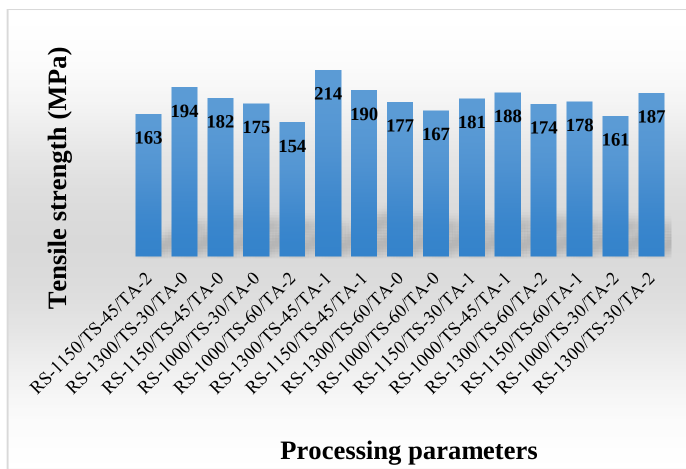

Figure 3: Comparison of tensile strength

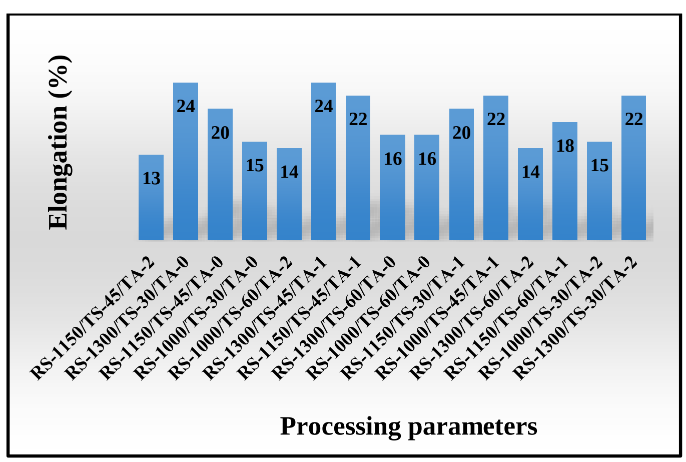

Figure 4: Comparison of percentage elongation

Table 3: Input processing parameters and their responses

Run	A:Tool Rotation Speed (rpm)	B:Traverse speed (mm/min)	C:Tilt Angle (°)	Tensile Strength (MPa)	Strain (%)	Hardness at Nugget (HV)	Residual Stress at Nugget (MPa)
1	1150	45	2	163	13	66	38
2	1300	30	0	194	24	83	24
3	1150	45	0	182	20	75	25
4	1000	30	0	175	15	70	33
5	1150	45	1	195	21	81	14
6	1000	60	2	154	14	61	44
7	1300	45	1	214	24	86	12
8	1150	45	1	192	22	80	15
9	1150	45	1	190	22	81	18
10	1300	60	0	177	16	73	29
11	1150	45	1	189	21	80	20
12	1000	60	0	167	16	66	36
13	1150	30	1	181	20	75	26
14	1150	45	1	187	21	78	21
15	1000	45	1	188	22	79	23
16	1300	60	2	174	14	68	35
17	1150	60	1	178	18	73	27
18	1000	30	2	161	15	63	40
19	1150	45	1	188	23	82	28
20	1300	30	2	187	22	76	22

3.2 Micro-hardness at Nugget zone

Fig. 5 shows the variation between micro-hardness and processing parameters of the friction stir welded joint of AA5083 and AA6082. Although the investigation of the microhardness across the weldment of AA5083 and AA6082 has been reported earlier [20]. The stirred zone (SZ) of friction stir welding have the highest hardness in the welded zone due to the high temperature which results in the dissolution of the precipitation phase in that zone. This increase in the hardness at the stirred zone was observed in friction stir welding of other precipitation hardened alloys [21].

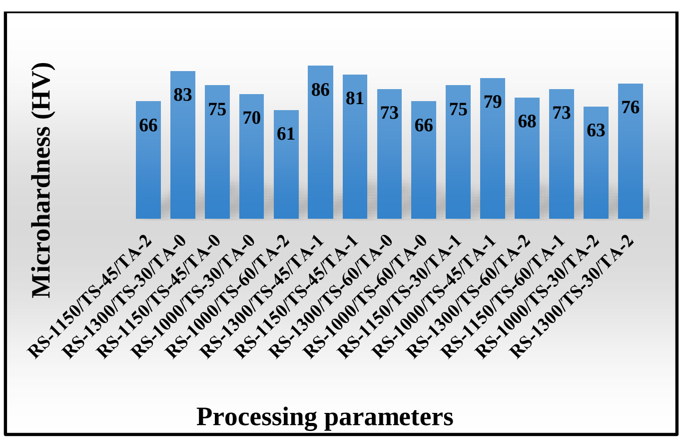

Figure 5: Variation of micro-hardness and processing parameters at nugget zone

The hardness values are depending on the precipitates distribution, grain size and dislocation structure. All welded samples, hardness decreases from thermo mechanically affected zone to the parent metal. This was happened that the temperature reached in the thermo mechanically affected zone to heat affected zone was sufficient for the ageing precipitate to be dissolved. The maximum micro-hardness (86 HV) was found at the processing parameter of rotation speed of 1300 rpm, traverse speed 45 mm/min with tilt angle 1^0, whereas the minimum micro-hardness (61 HV) was found at the processing parameter of rotation speed of 1000 rpm, traverse speed 60 mm/min with tilt angle 2^0

3.3 Residual stress at Nugget zone

Residual stress measurement and control are very important for the safety of structures of high-speed trains, and airplane wings, which is critical for the structure design. Residual stresses can be tensile or compressive depending up on the location and type of non-uniform volumetric change taking place. Differential heating or cooling in welding and heat treatment, or localized stresses like in contour rolling, machining and shot peening can result in residual stresses. We measured the Friction Stir Welded plates at ambient temperature to identify the tensile and compressive stresses at particular locations in the transverse and longitudinal directions which affect the mechanical properties of the joint at different process parameters.There are two types of residual stress found in the weldment, usually tensile residual stress located in the weld area, whereas compressive residual stress can be found at heat affected zone. It is found that the residual at the center of the weldment decreases with increases the tool rotational speed. The maximum compressive residual stress (44 MPa) was found at tool rotational speed of 1000 rpm, traverse speed 60 mm/min with tilt angle 2^0, whereas the minimum compressive residual stress 12 MPa was found at tool rotational speed of 1300 rpm, traverse speed 45 mm/min with tilt angle 1^o as shown in fig. 6. It was found that in the region where the equivalent plastic strain is increases, the residual stress is decreases. When away from the stir zone point of the welded joint, the residual stress is slightly increases but after stir zone the distribution of residual stress remains almost steady. Because of unsymmetrical deformation at the welding zone, the residual stresses are not symmetric to the welding line. When the fixture is released and the temperature is going to reduce to room temperature then the material in the nugget zone tends to recover. But the weldment in the HAZ has smaller deformation and will prevent the recovery process in the nugget zone. So the maximum residual stress (RS) occur in the boundaries of the heat affected zone (HAZ) and minimum in the nugget zone (NZ).

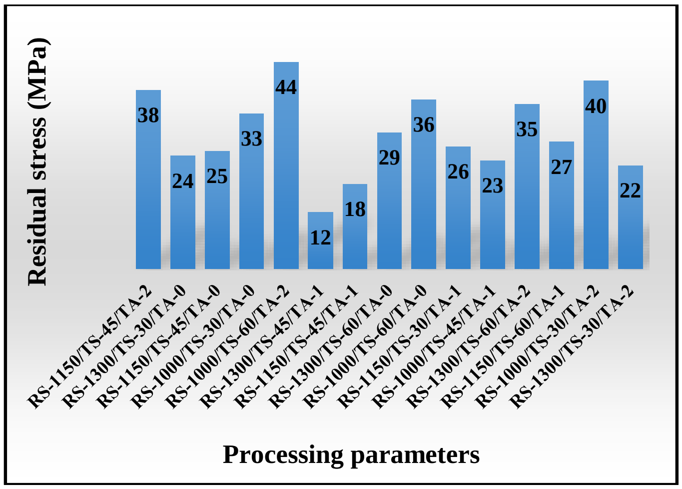

Figure 6: Variation of micro-hardness and processing parameters at nugget zone

3.4 Evaluating the adequacy of the developed model

The empirical relationship for the output responses i.e. tensile strength, micro-hardness and residual stress has been developed and the adequacy was analyzed by response surface methodology (RSM) technique. The FSW experiments were designed with the help of design expert software with 20 experiments. To identify the process parameters that are statistically significant, analysis of variance (ANOVA) test was conducted. The purpose of ANOVA test is to determine the significance of process parameters which affect the mechanical properties of friction stir welded joints. The F-test (Fisher's test) may also be used to determine which process parameter has a significant effect on the mechanical properties. The results of ANOVA test show that the opt process parameters are highly significant factor affecting the mechanical properties of friction stir welded joint in order to tool rotational speed, traverse speed and tilt angle. The developed models were tested using ANOVA method with the help of design expert software. The ANOVA results for tensile strength, percentage elongation and hardness at nugget zones are shown in table 4-6. The all models give the highly significant fisher's F value which shows that the model adequately representing the relationship between process parameters and response. The fisher's F value of developed model for tensile strength is 26.67 which shows that the model is significant and there is only 0.01% chance that a model Fisher's value could occur due to noise. The lack of fit F value of 2.28 shows that the lack of fit is not significant. For a good model lack of fit should be not significant. The residual error value (150.93) should be the sum of lack of fit (104.96) and pure error (46). By this column of fit summary recommended quadratic model is statically significant for analyzing the tensile stress of welded joint of AA5083 and AA6082. The fisher's F value of developed model for percentage elongation is 12.51 which shows that the model is significant and there is only 0.02% chance that a model Fisher's value could occur due to noise. The lack of fit F value of 5.18 shows that the lack of fit is not significant. For a good model lack of fit should be not significant. The residual error value (20.6) should be the sum of lack of fit (17.27) and pure error (3.33). By this column of fit summary recommended quadratic model is statically significant for analyzing the percentage elongation of welded joint of AA5083 and AA6082. The fisher's F value of developed model for micro-hardness at nugget zone is 36.13 which shows that the model is significant and there is only 0.01% chance that a model Fisher's value could occur due to noise. The lack of fit F value of 2.09 shows that the lack of fit is not significant. For a good model lack of fit should be not significant. The residual error value (28.8) should be the sum of lack of fit (19.47) and pure error (9.33). By this column of fit summary recommended quadratic model is statically significant for analyzing the micro-hardness at nugget zone of welded joint of AA5083 and AA6082. The fisher's F value of developed model for residual stress at nugget zone is 8.34 which shows that the model is significant and there is only 0.13% chance that a model Fisher's value could occur due to noise. The lack of fit F value of 0.8298 shows that the lack of fit is not significant. For a good model lack of fit should be not significant. By this column of fit summary recommended quadratic model is statically significant for analyzing the residual stress at nugget zone of welded joint of AA5083 and AA6082.

3.5 Developing a mathematical model

The empirical relationship was developed for the response variable i.e. ultimate tensile strength, percentage elongation, and micro-hardness and residual stress at nugget zone under the input processing parameters i.e. tool rotational speed (A), traverse speed (B) and tilt angle (c) using analysis of variance technique with the help of design expert software. The mathematical empirical relationship for tensile strength, percentage elongation and micro-hardness at nugget zone are as follow.

$$\text{Tensile strength} = 696.7 - 1.12A + 4.67B + 8.56C - 0.00083AB + 0.0175\,AC + 0.04167\,BC + 0.00052A^2 - .0452\,B^2 - 18.18C^2$$

$$\text{Strain (\%)} = 60.68 - 0.15A + 1.71B + 10.36C - 0.00088AB - 0.0017AC - 0.0167BC - 0.0089B^2 - 4.5C^2$$

$$\text{Microhardness} = 174.09 - 0.296A + 2.56B + 12.2C - 0.00067AB + 0.033BC - 00016A^2 - 0.022B^2 - 8.5C^2$$

$$\text{Residual stress} = 55.32 + 0.28A - 2.895B - 11.08C + 0.00061AB - 0.00916AC + 0.075BC - 0.000145A^2 + 0.0254B^2 + 10.72C^2$$

Table 4: analysis of variance (ANOVA) test for tensile strength

Tensile Strength						
Source	Sum of Squares	df	Mean Square	F-value	p-value	
Model	3622.27	9	402.47	26.67	< 0.0001	significant
A-Tool Rotation Speed	1000	1	1000	66.25	< 0.0001	significant
B-Traverse speed	230.4	1	230.4	15.26	0.0029	significant
C-Tilt Angle	336.4	1	336.4	22.29	0.0008	significant
AB	28.13	1	28.13	1.86	0.2022	significant
AC	55.13	1	55.13	3.65	0.0851	significant
BC	3.13	1	3.13	0.207	0.6588	significant
A^2	384.09	1	384.09	25.45	0.0005	significant
B^2	285.09	1	285.09	18.89	0.0015	significant
C^2	909.09	1	909.09	60.23	< 0.0001	significant
Residual	150.93	10	15.09			
Lack of Fit	104.93	5	20.99	2.28	0.1932	not significant
Pure Error	46	5	9.2			
Cor Total	3773.2	19				

Table 5: analysis of variance (ANOVA) test for percentage elongation

% Elongation						
Source	Sum of Squares	df	Mean Square	F-value	p-value	
Model	231.95	9	25.77	12.51	0.0002	significant
A-Tool Rotation Speed	32.4	1	32.4	15.73	0.0027	significant
B-Traverse speed	32.4	1	32.4	15.73	0.0027	significant
C-Tilt Angle	16.9	1	16.9	8.2	0.0168	significant
AB	32	1	32	15.53	0.0028	significant
AC	0.5	1	0.5	0.2427	0.6329	significant
BC	0.5	1	0.5	0.2427	0.6329	significant
A^2	11	1	11	5.34	0.0434	significant
B^2	11	1	11	5.34	0.0434	significant
C^2	55.69	1	55.69	27.03	0.0004	significant
Residual	20.6	10	2.06			
Lack of Fit	17.27	5	3.45	5.18	0.0476	Not significant
Pure Error	3.33	5	0.6667			
Cor Total	252.55	19				

Table 6: analysis of variance (ANOVA) test for micro-hardness at nugget zone

Micro-Hardness						
Source	Sum of Squares	df	Mean Square	F-value	p-value	
Model	936.4	9	104.04	36.13	< 0.0001	significant
A-Tool Rotation Speed	220.9	1	220.9	76.7	< 0.0001	significant
B-Traverse speed	67.6	1	67.6	23.47	0.0007	significant
C-Tilt Angle	108.9	1	108.9	37.81	0.0001	significant
AB	18	1	18	6.25	0.0314	significant
AC	0	1	0	0	1	significant
BC	2	1	2	0.6944	0.4241	significant
A^2	33.69	1	33.69	11.7	0.0065	significant
B^2	68.75	1	68.75	23.87	0.0006	significant
C^2	198.69	1	198.69	68.99	< 0.0001	significant
Residual	28.8	10	2.88			
Lack of Fit	19.47	5	3.89	2.09	0.2195	not significant
Pure Error	9.33	5	1.87			
Cor Total	965.2	19				

3.6 Influence of process parameters on tensile strength, micro-hardness and residual stress

Response surface method (RSM) is used an optimization tool to obtained the optimum values of the process parameters. Design expert software is used to optimize the process parameters. For this purpose, contour plots and 3D response surface graph are made based on the model developed by considering the optimum process parameters. The optimum tensile strength, percentage elongation and micro-hardness at nugget zone of friction stir welding joint of AA5083 and AA6082 is exhibited by the peak of response surface as shown in fig.7-9. When the tool rotational speed increases, then the tensile strength also increases due to strain hardening effect induced by tool stirring, whereas excess heat input play the predominant role at high tool rotation speed such lower tensile strength was observed when the tool rotation increases. As the feed rate increases then tensile strength first increases then decreases as shown in fig. 7. The minimum tensile strength was found at lower tool rotation speed due to inadequate tool stirring action [22]. The maximum tensile strength (214 MPa) was observed at tool rotation 1300 rpm, traverse speed 45 mm/min with tilt angle 1^0.

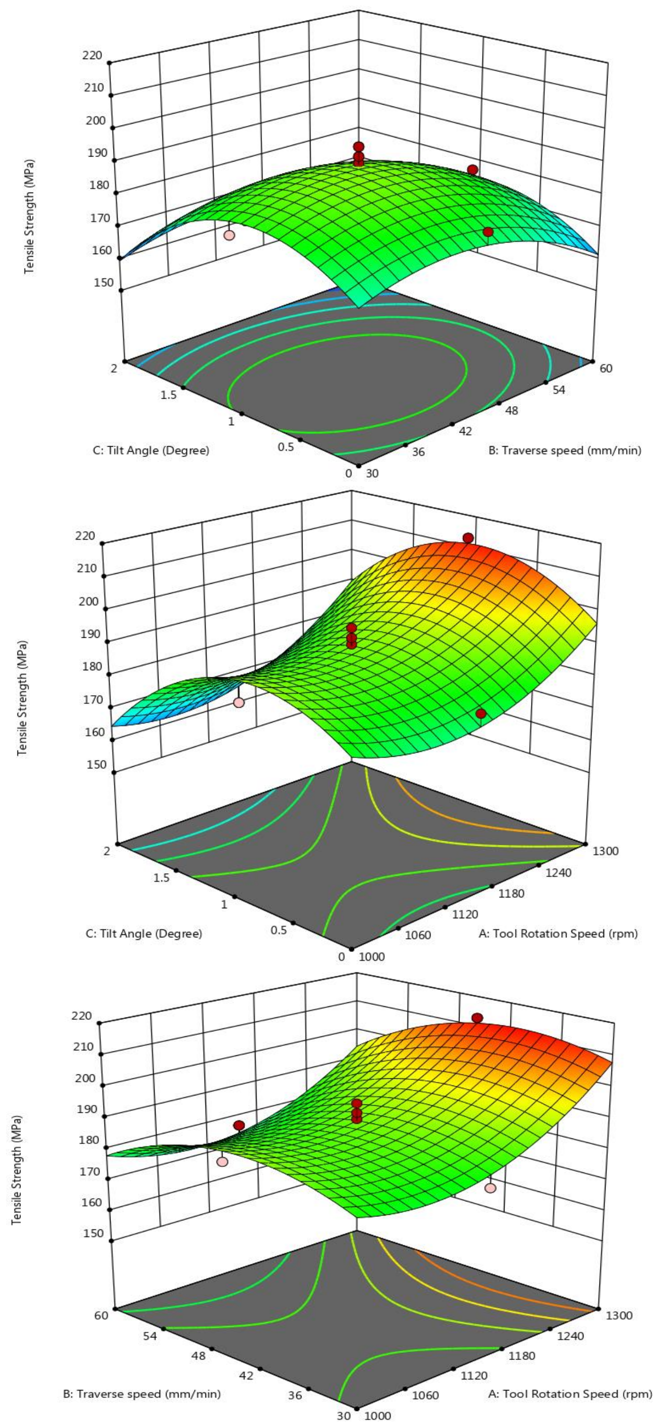

Figure 7: 3D response surface plot and contour plot for tensile strength of FSW joint of AA5083 and AA6082

When the feed rate or traverses speed increases, the tensile strength and hardness also increases up to a certain value. Large heat was found in the welded region at lower welding traverse speed. As the traverse speed increases, the effect of thermal cycle on the welded joint properties is weakened leading to an improvement in tensile strength and hardness of the welded joint.

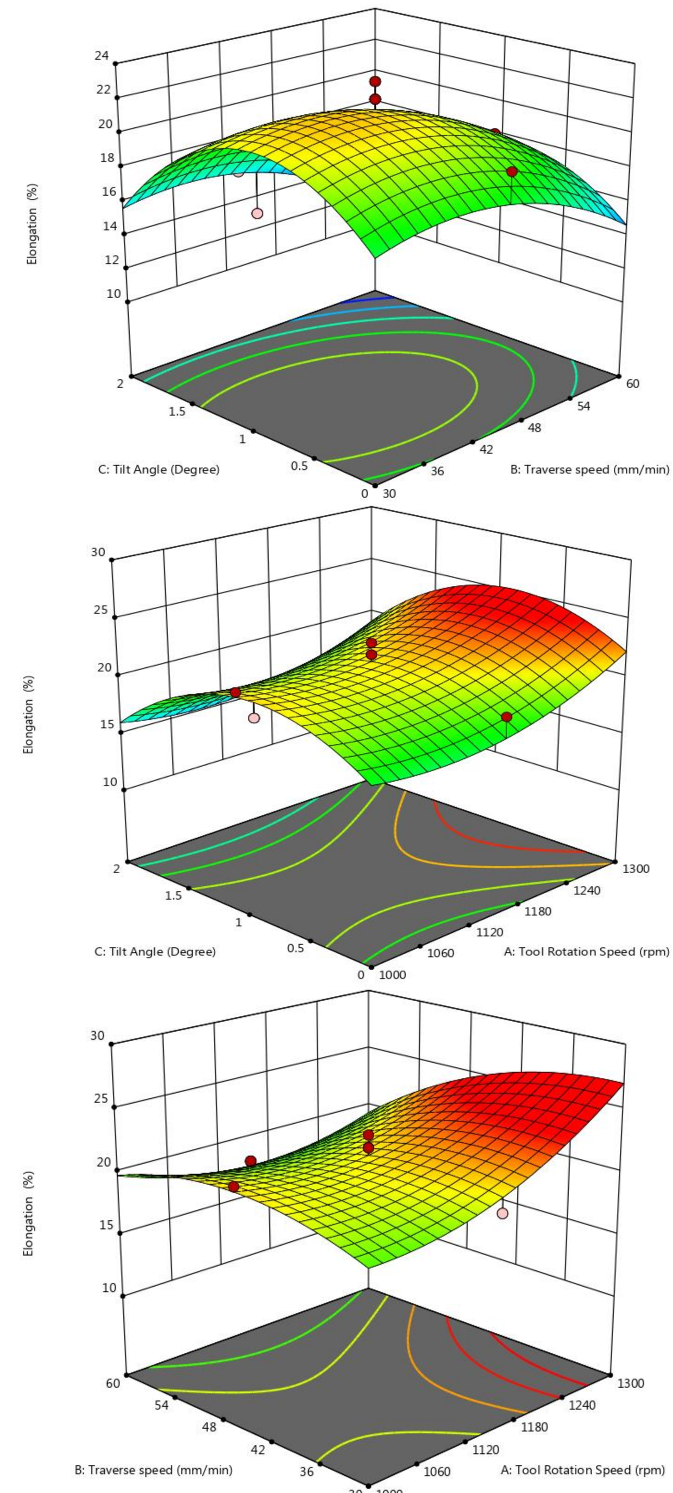

Figure 8: 3D response surface plot and contour plot for percentage elongation of FSW joint of AA5083 and AA6082

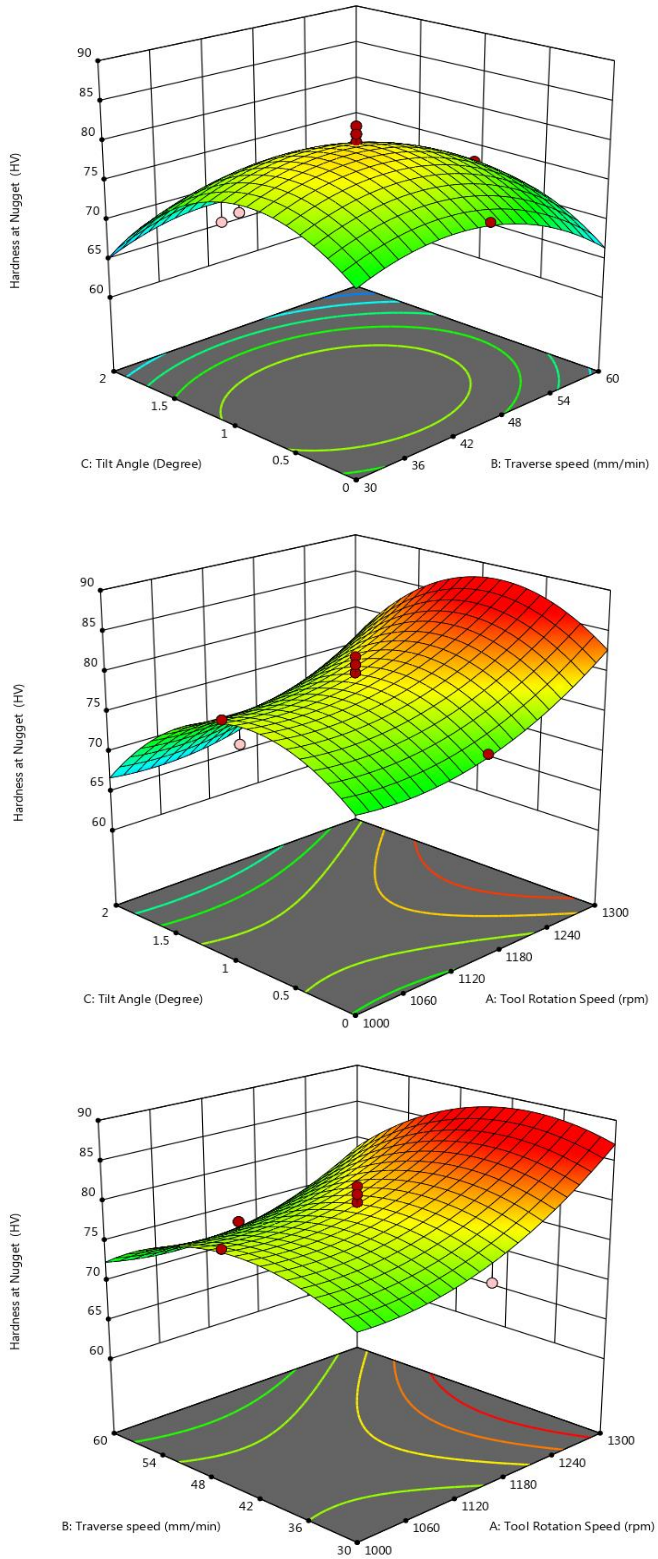

Figure 9: 3D response surface plot and contour plot for micro-hardness at nugget zone of FSW joint of AA5083 and AA6082

3.7 Effect of process parameters on response variables

Fig. 10-11, shows the variation of response parameters and processing parameters of FSW welded joint of AA5083 and AA6082. According to these figures when the tool rotation increases, response parameters (tensile strength, percentage elongation and micro-hardness at nugget zone) also increases at certain limit, whereas when traverse speed increases the response parameters first increases then decreases and when tilt angle is increases, response parameters first decreases then increases at tilt angle 2^0 as shown in fig. 10-11.

When the tool rotational speed is compared with the tilt angle and traverse speed then the rotational speed is more sensitive to change or increase the tensile strength and micro-hardness of the friction stir welded joint of AA5083 and AA6082 because the heat generation is mainly depended on tool rotational speed, higher tool rotational speed produces higher heat generation [23]. The cube function graph of multi response optimization as shown in fig. 10-11. This methodology is used to optimize for more than one objective function. The desirable value is 1 for optimized value of the input processing parameters and responses. The optimized value of tensile strength, percentage elongation, micro-hardness at nugget zone and residual stress at nugget zone are 187.6 MPa, 19.93, 78.39 HV and 22.02 MPa respectively, whereas the optimized value of tool rotational speed, feed rate and tilt angle are 1227.7 rpm, 53.20 mm/min and 0.3741 respectively as shown in fig. 12.

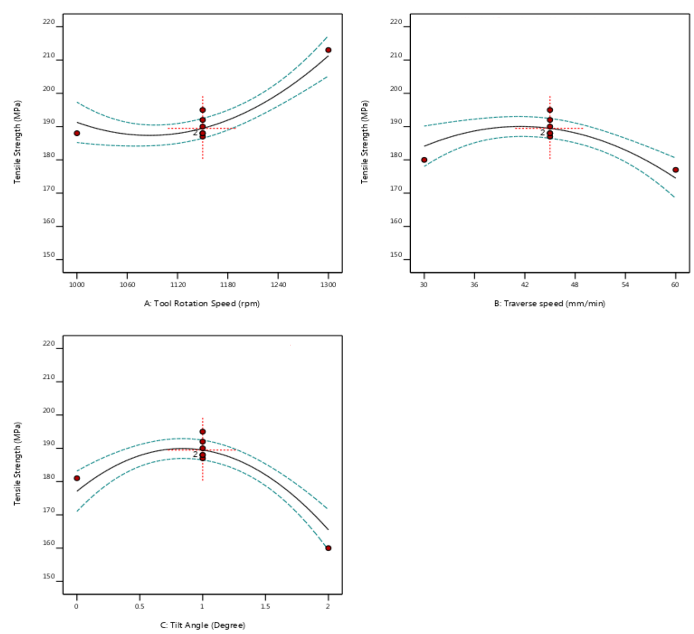

Figure 10: Variation of Tensile strength and processing parameters of welded joint of AA5083 and AA6082

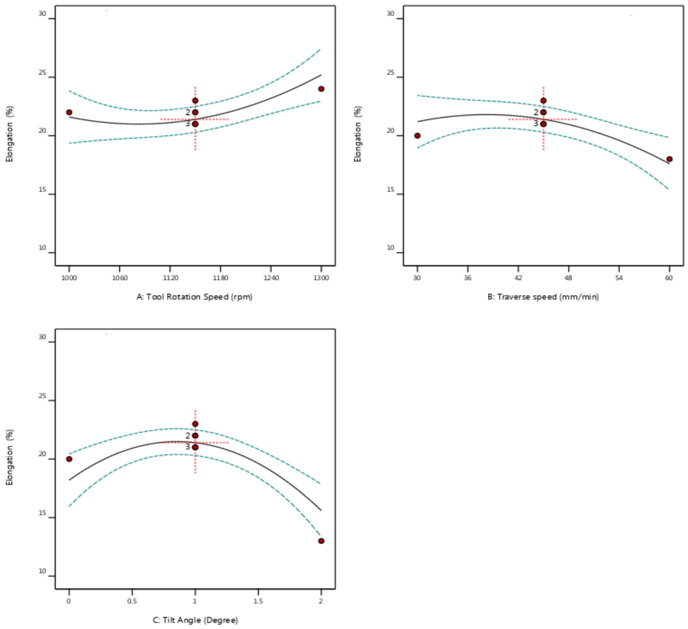

Figure 11: Variation of percentage elongation and processing parameters of welded joint of AA5083 and AA6082

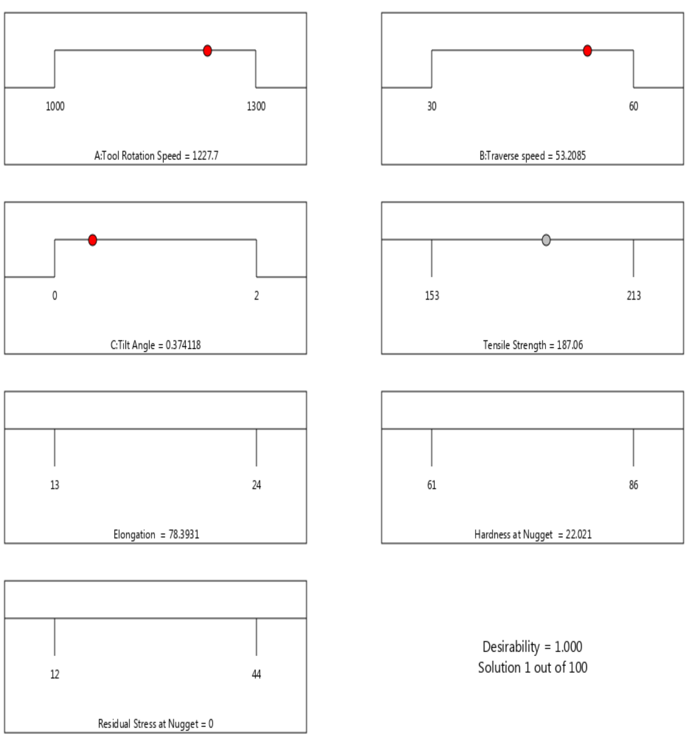

Figure 12: Ramp chart with optimized FSW parameters for output responses

4. Conclusions

The present work was design to optimize the processing parameters of friction stir welded joints of dissimilar aluminum alloy of AA5083 and AA6082 and the following conclusions have been made.

- Friction stir welding of dissimilar aluminum alloys AA5083 and AA6082 aluminum alloys of 6 mm plates have been welded.
- The experiments were designed with the help of CCD of RSM and the FSW parameters such as tool rotational speed, traverse speed and tilt angle were considered.
- The maximum tensile strength (214 MPa) was found at tool rotation speed 1300 rpm, traverse speed 45 mm/min with tilt angle 1^0
- The maximum micro-hardness (86 HV) was found at tool rotation speed 1300 rpm, traverse speed 45 mm/min with tilt angle 1^0
- The minimum tensile strength (161 MPa) was observed at tool rotation speed 1000 rpm, traverse speed 30 mm/min with tilt angle 2^0.
- In addition, a numerical model and empirical relationship was developed by design expert software between processing parameters (tool rotation speed, traverse speed, and tilt angle) and response surface parameters (tensile strength, percentage elongation and micro-hardness at nugget zone) and the optimized value of tensile strength, % elongation, micro-hardness, and residual stress were observed as 187.6 MPa, 19.93, 78.39 HV and 22.02 MPa respectively.

References

[1] Husain Mehdi, R.S. Mishra, An experimental analysis and optimization of process parameters of AA6061 and AA7075 welded joint by TIG+FSP welding using RSM, Advances in Materials and Processing Technologies, 2020, https://doi.org/10.1080/2374068X.2020.1829952.

[2] G. Buffa, J.Hua, R. Shivpuri, L. Fratini, A continuum based fem model for friction stir welding—model development, Materials Science and Engineering A 419 (2006) 389–396.

[3] Judy Schneider, Ronald Beshears, Arthur C. Nunes Jr, Interfacial sticking and slipping in the friction stir welding process, Materials Science and Engineering A 435–436 (2006) 297–304.

[4] Adamowski, J., C. Gambaro, E. Lertora, M. Ponte, and M. Szkodo. "Analysis of FSW welds made of aluminium alloy AW6082-T6", Archives of Materials Science and Engineering, 28, no. 8 (2007): 453-460.

[5] Husain Mehdi, R.S Mishra (2016), Mechanical Properties and Microstructure Studies in Friction Stir Welding (FSW)Joints of Dissimilar Alloy-A Review, Journal of Achievements of Materials and Manufacturing Engineering , vol-77, issue1, pp 31-40.

[6] Husain Mehdi, R.S. Mishra (2019), Analysis of Material Flow and Heat Transfer in Reverse Dual Rotation Friction Stir Welding: A Review, International Journal of Steel Structure, vol-19, issue-2, pp 422-434.

[7] Husain Mehdi, R.S. Mishra (2019), Study of the influence of friction stir processing on tungsten inert gas welding of different aluminum alloy, SN Applied Sciences, vol-1, issue-7, 712.

[8] Husain Mehdi, R.S. Mishra (2020), Investigation of mechanical properties and heat transfer of welded joint of AA6061 and AA7075 using TIG+FSP welding approach, Journal of Advanced Joining Processes, vol-1, issue-1, 100003.

[9] Husain Mehdi, R.S. Mishra (2020), Effect of Friction Stir Processing on Microstructure and Mechanical Properties of TIG Welded Joint of AA6061 and AA7075, Metallography, Microstructure, and Analysis, vol-9, 403-418.

[10] Husain Mehdi, R.S. Mishra (2020), Effect of friction stir processing on mechanical properties and heat transfer of TIG-welded joint of AA6061 and AA7075, Defence Technology. https://doi.org/10.1016/j.dt.2020.04.014.

[11] Husain Mehdi, R.S. Mishra (2020), Influence of friction stir processing on weld temperature distribution and mechanical properties of TIG

welded joint of AA6061 and AA7075 Transactions of the Indian Institute of Metals, vol-73, 1773-1788.

[12] A.Nait Salah, M. Kaddami, Husain Mehdi, Mechanical Properties And Microstructure Characterization of Friction Stir Welded Joint Of Dissimilar Aluminum Alloy AA2024 And AA7050, Turkish Journal of Computer and Mathematics Education, 12(7), 1051-1061 (2021).

[13] Cam, Gürel, and Selcuk Mistikoglu. "Recent developments in friction stir welding of Al-alloys." Journal of Materials Engineering and Performance 23, no. 6 (2009): 1936-1953.

[14] DebRoy, T., and Bhadeshia H. K. D. H.. "Friction stir welding of dissimilar alloys–a perspective." Science and Technology of Welding and Joining 15, no. 4 (2010): 266-270.

[15] Husain Mehdi, R.S. Mishra, Microstructure and mechanical characterization of tungsten inert gas-welded joint of AA6061 and AA7075 by friction stir processing, Proceedings of the Institution of Mechanical Engineers, Part L: Journal of Materials: Design and Applications, 235 (11), 2531-2546 (2021), https://doi.org/10.1177/14644207211007882.

[16] Hassen Bouzaiene, Mohamed-Ali Rezgui, Mahfoudh Ayadi, Ali Zghal, Correlation between welding and hardening parameters of friction stir welded joints of 2017 aluminum alloy, Trans. Nonferrous Met. Soc. China 22(2012) 1064-1072.

[17] Varun Kumar, A., and Balachandar K. "Effect of welding parameters on metallurgical properties of friction stir welded aluminium alloy 6063-O." Journal of Applied Sciences 12 (2012): 1255-1264.

[18] Azimzadegan T, Serajzadeh S. An Investigation into microstructures and mechanical properties of AA7075-T6 during friction stir welding at relatively high rotational speeds [J]. Journal of Materials Engineering Performance, 2010, 19(9): 1256−1263.

[19] Husain Mehdi, R.S. Mishra, Effect of Friction Stir Processing on Mechanical Properties and Wear Resistance of Tungsten Inert Gas Welded Joint of Dissimilar Aluminum Alloys. Journal of Materials Engineering and Performance volume, 30, 1926–1937 (2021). https://doi.org/10.1007/s11665-021-05549-y

[20] Donatus U, Thompson G E, Zhou X, Wang J, Beamish K. Flow patterns in friction stir welds of AA5083 and AA6082 alloys [J]. Materials & Design, 2015, 83: 203−213.

[21] M.M.Z. Ahmeda, B.P. Wynnea, W.M. Rainfortha, P.L. Threadgill, Microstructure, crystallographic texture and mechanical properties of friction stir welded AA2017A, Mater. Charact. 64 (2012) 107–117.

[22] Husain Mehdi, Anil Kumar, Arshad Mahmood, Manoj Saini, Experimental Analysis of Mechanical Properties of Composite Material Reinforced by Aluminium-Synthetic Fibers, 2(4), 2014, 59-69..

[23] Rajakumar R, Muralidharan C, Balasubramanian V. Influence of friction-stir-welding process and tool parameters on strength properties of AA7075-T6 aluminium alloy joints [J]. Material Design, 2011, 32: 535-543.

Cite this article as: Muzamil Farooq, Amit Gupta, Vikas Nandal, Optimization of process parameters of friction stir welded joint of dissimilar aluminum alloy AA5083 and AA6082, International journal of research in engineering and innovation (IJREI), vol 5, issue 1 (2020), 10-19. *https://doi.org/10.36037/IJREI.2021.5102*.